Eur. Phys. J. B **30**, 33–38 (2002)
DOI: 10.1140/epjb/e2002-00354-y

THE EUROPEAN PHYSICAL JOURNAL B

Coexistence of superconductivity and ferromagnetism in ferromagnet/superconductor proximity structures

Guoya Sun[1], D.Y. Xing[1,a], R. Shen[1], and H.Q. Lin[2]

[1] National Laboratory of Solid State Microstructures and Department of Physics, Nanjing University, Nanjing 210093, PR China
[2] Department of Physics, The Chinese University of Hong Kong, Hong Kong, PR China

Received 1st July 2002
Published online 19 November 2002 –

Abstract. The Nambu spinor Green's function approach is applied to calculating the density of states (DOS) and superconducting order parameter in normal-metal/insulator/ferromagnet/superconductor (NM/I/FM/SC) junctions. It is found that the s-wave superconductivity and ferromagnetism can coexist near the FM/SC interface, which is induced by proximity effect. On the SC side, the spin-dependent DOS appears both within and without the energy gap. On the FM side, the superconducting order parameter displays a damped oscillation and the DOS exhibits some superconducting behavior. The calculated result for the DOS in FM for "0 state" and "π state" can reproduce recent tunneling spectra in $Al/Al_2O_3/PdNi/Nb$ tunnel junctions.

PACS. 74.50.+r Proximity effects, weak links, tunneling phenomena, and Josephson effects – 74.80.Fp Point contacts; SN and SNS junctions – 74.80.-g Spatially inhomogeneous structures

Coexistence of superconductivity and ferromagnetism has been a most interesting subject in the condensed matter physics for a long time. The early investigation traces back to original works in the sixties by Clogston [1], Chandrasekhar [2], Abrikosov and Gorkov [3], Fulde and Ferrel [4], and Larkin and Ovchinnikov [5]. These works focused on the spin-singlet superconductivity in a bulk metal with a spin-exchange field, such as produced by ferromagnetically aligned impurities. The presence of the exchange field is unfavorable to the spin-singlet superconductivity. Only when the exchange energy h_0 is small enough, being of the same order of magnitude as the superconducting energy gap Δ_0, the spin-singlet superconductivity remains existing. In the s-wave case, for $h_0/\Delta_0 < 0.707$ all the itinerant electrons near the Fermi level form the Cooper pairs with opposite spins and zero center-of-momentum [1]; while for $0.707 < h_0/\Delta_0 < 0.754$ part of the itinerant electrons near the Fermi level form the Cooper pairs with finite center-of-mass momentum and unpaired electrons show a finite magnetization, which is usually called the FFLO state [4,5]. In a bulk ferromagnet (FM) h_0 is typically at least 2 orders of magnitude larger than Δ_0 of a bulk superconductor (SC), so that the "FFLO" state has never been observed in bulk materials. However, this condition required for coexistence of spin-singlet superconductivity and ferromagnetism may be largely relaxed in an FM/SC structure, where the Cooper pairs are injected from SC into FM by proximity effect and the spin-polarized electrons (holes) are injected from FM into SC. Very recently, it has been shown that inhomogeneous superconductivity can be induced by the proximity effect in a thin FM film in contact to an SC [6] and a weak FM sandwiched between two SCs [7], even though h_0 in FM is much greater than Δ_0 in SC.

In the FM/SC structure the injection of the Cooper pairs from SC into FM gives rise to superconducting order parameter in FM near the FM/SC interface. With increasing the distance from the interface, the induced superconductivity order parameter in FM exhibits a damped oscillation, and its sign reverses from positive to negative, corresponding to a transition from the "0 state" to "π state". Kontos *et al.* [6] measured the tunneling spectroscopy of $Al/Al_2O_3/PdNi/Nb$ tunnel junctions, which corresponds to the density of states (DOS) in PdNi at the Al_2O_3/PdNi interface. It is found that the DOS exhibits an induced superconducting feature. As the thickness of PdNi is increased from 50 to 75 Å, the induced superconducting DOS is reversed with respect to the normal state, accompanied by a change from the "0 state" to "π

[a] e-mail: dyxing@nju.edu.cn

state". Ryazanov *et al.* [7] measured the critical current through an $Nb/Cu_{0.48}Ni_{0.52}/Nb$ Josephson junction and found nonmonotonic dependence on temperature, which can be interpreted in terms of a π-phase shift due to the exchange splitting. On the theoretical side, Buzdin [8] used the Usadel equation in the dirty limit to obtain damped-oscillatory behavior of the DOS close to the Fermi level in an FM near the boundary with an SC. Zareyan *et al.* [9] used a quasiclassical approach based on the Eilenberger equation in the clean limit to reproduce the DOS within the energy gap, which had been observed in either "0" or "π state" [6]. These experimental data for DOS in FM were further reproduced in the energy range of $E < 4\Delta_0$ by Sun *et al.* [10] in the Nambu spinor Green's function approach based on the pioneer works of McMillan [11] and Blonder, Tinkham, and Klapwijk (BTK) [12]. In particular, the peak in DOS at $E = \Delta_0$ for the "0 state" and the dip in DOS at the same energy for the "π state" were well reproduced. Two approximations were made in the approach of reference [10]. One is to apply the one-dimensional (1D) BTK theory to the real 3D interface system, so that the virtual Andreev reflection [13,14] special for the FM/SC interface is not explicitly taken into account. The other is to replace a finite FM thin film in the real FM/SC system [6] with a semi-infinite FM. Although the two approximations have been argued to be reasonable, their justification is highly required by calculating the tunneling spectroscopy of a real system measured in the experiment.

In this paper we focus on possible coexistence of ferromagnetism and superconductivity in the regions near the FM/SC interface. The system under consideration is an NM/I/FM/SC structure where NM indicates a nonmagnetic metal electrode and I stands for an insulating thin film. This system corresponds just to the $Al/Al_2O_3/PdNi/Nb$ tunnel junction in the experiment of Kontos *et al.* [6], in which the PdNi/Nb junction is the principle part and $Al/Al_2O_3/PdNi$ tunnel junction is used to measure the DOS in PdNi at the $Al_2O_3/PdNi$ interface. The proximity effect found in the present system is twofold. On the SC side, there is finite DOS within the energy gap ($E < \Delta_0$), exhibiting gapless superconductivity. More importantly, the finite DOS in SC is shown to be spin dependent, indicating that there exists weak ferromagnetism in SC near the interface. Although the gapless state in the superconducting region close to an SC/NM interface has already been obtained [15,16], the present study on the DOS in the FM/SC proximity structure gives richer gapless effects. On the FM side, the DOS exhibits the superconducting feature. The calculated results for the DOS, which are obtained from a 3D extension of the BTK theory and the Nambu spinor Green's function approach, are quantitatively consistent with the experimental data [6].

Consider an NM/FM/SC system with a semi-infinite NM to the left of $x = -L/2$, a semi-infinite SC to the right of $x = L/2$ and an FM thin film between $x = -L/2$ and $L/2$, as shown in Figure 1a. The NM/FM and FM/SC interfaces are described by two δ-functions:

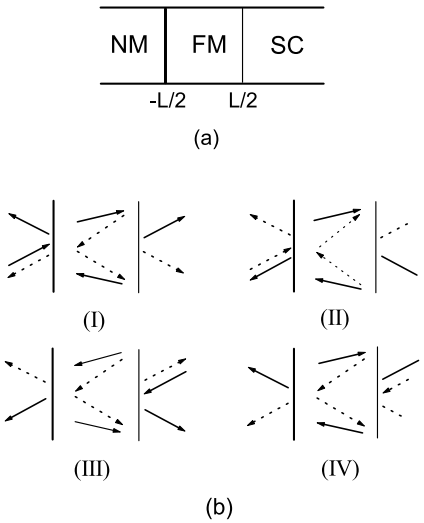

Fig. 1. Schematic illustration of NM/I/FM/SC structure (a) and quasiparticle injection processes (b) in NM/I/FM/SC structure. The solid-line arrow stands for the electron in FM and NM or electronlike quasiparticle in SC with spin σ, while the dashed-line arrow for the hole in FM and NM or holelike quasiparticle in SC with spin $\overline{\sigma}$.

$U_1\delta(x+L/2)+U_2\delta(x-L/2)$, where U_1 and U_2 indicate the strength of two interface potential barriers, respectively. In order to simulate the $Al/Al_2O_3/PdNi/Nb$ tunnel junction [6], in the numerical calculations, U_1 will be taken to be a large value and U_2 to be a small one, respectively, describing the insulating Al_2O_3 thin film and a very low PdNi/Nb interface resistance. The FM film is described by an effective single-particle Hamiltonian with exchange energy h_0, and the SC is assumed s-wave pairing and described by a BCS-like Hamiltonian. Owing to the interplay between FM and SC the BCS pair potential near the interface should be determined in a self-consistent way. As a reasonable guess for the self-consistent pair potential, we choose $\Delta(x) = \Delta_0\Theta(x - L/2)$ with Δ_0 the energy gap of the bulk SC and $\Theta(x)$ is the unit step function. [11] In general, the quasiparticle wave function should satisfy the four-component BdG equation, for the wave function has four components, respectively, for electronlike quasiparticle (ELQ) and holelike quasiparticle (HLQ) with spin up and down. In the absence of spin-flip scattering, however, the four-component BdG equations may be decoupled into two sets of two-component equations: one for the spin-up electronlike and spin-down holelike quasiparticle wave functions $(u_\uparrow, v_\downarrow)$, the other for $(u_\downarrow, v_\uparrow)$. [10] Following the standard method developed by McMillan [11], we employ two envelop functions that are smooth on the atomic scale length, $\overline{u}_\sigma(\mathbf{r}) = u_\sigma(\mathbf{r})\exp(-\mathrm{i}\mathbf{k}_\mathbf{F}^\sigma \cdot \mathbf{r})$ and $\overline{v}_{\overline{\sigma}}(\mathbf{r}) = v_{\overline{\sigma}}(\mathbf{r})\exp(-\mathrm{i}\mathbf{k}_\mathbf{F}^{\overline{\sigma}} \cdot \mathbf{r})$. Here $\sigma = \uparrow$ and $\downarrow$ stand for the spin direction, and $\overline{\sigma}$ is the opposite to σ. In both SC and NM $k_F^\sigma = k_F$ is the spin-independent Fermi wavevector; and in FM $k_F^\sigma = k_F\sqrt{1+\eta_\sigma h_0/E_F}$ with $\eta_\sigma = 1$ for $\sigma = \uparrow$ and -1 for $\sigma = \downarrow$. By dropping the terms as $\partial^2/\partial x^2$ which are of order Δ_0/E_F with respect to the $\partial/\partial x$ term,

we obtain the reduced BdG equation for the quasiparticle wave function [11],

$$\frac{-\mathrm{i}\hbar^2 k_F^{\sigma}}{m}(\hat{\mathbf{k}}\cdot\nabla)\overline{u}_{\sigma}(\mathbf{r})+\overline{\Delta}^{*}(\mathbf{r})\overline{v}_{\overline{\sigma}}(\mathbf{r})=E\overline{u}_{\sigma}(\mathbf{r}), \quad (1)$$

$$\frac{\mathrm{i}\hbar^2 k_F^{\overline{\sigma}}}{m}(\hat{\mathbf{k}}\cdot\nabla)\overline{v}_{\overline{\sigma}}(\mathbf{r})+\overline{\Delta}(\mathbf{r})\overline{u}_{\sigma}(\mathbf{r})=E\overline{v}_{\overline{\sigma}}(\mathbf{r}), \quad (2)$$

where $\hat{\mathbf{k}}$ is a unit vector denoting the direction of wavevector $\mathbf{k}$, $\overline{\Delta}(\mathbf{r})=\Delta(\mathbf{r})\exp[\mathrm{i}(\mathbf{k}_{\mathbf{F}}^{\sigma}-\mathbf{k}_{\mathbf{F}}^{\overline{\sigma}})\cdot\mathbf{r}]$, and E is the quasiparticle energy relative to the Fermi energy E_F.

At the FM/SC interface there are four types of quasiparticle injection processes: electron and hole injection from FM to SC, and electronlike quasiparticle (ELQ) and holelike quasiparticle (HLQ) injection from SC to FM. If the spin degree of freedom is considered, there may be eight types of quasiparticle injection. Consider an electron with spin-σ incident on the interface from FM at an angle θ_{FN} to the interface normal. There are four possible trajectories: normal reflection (NR) at θ_{FN} and Andreev reflection (AR) [17] as a hole with spin-$\overline{\sigma}$ at angle θ_{FA} in FM; and transmission to SC as ELQ with spin-σ and HLQ with spin-$\overline{\sigma}$ at angle θ_S. In FM wave vectors of electrons with different spin, k_F^{σ} and $k_F^{\overline{\sigma}}$, are not equal due to the presence of the exchange energy h_0; also, neither of them is equal to k_F in SC. In the BTK approach the wave-vector component parallel to the interface is assumed to remain unchanged in the reflection and transmission processes, *i.e.*, they must satisfy the condition: $k_F^{\sigma}\sin\theta_{FN}=k_F^{\overline{\sigma}}\sin\theta_{FA}=k_F\sin\theta_S$. As a result, θ_{FN}, θ_{FA}, and θ_S differ from each other except when θ_{FN} equals zero. For example, since $k_F^{\uparrow}>k_F>k_F^{\downarrow}$, we have $\theta_{FN}<\theta_S<\theta_{FA}$ for the incident electrons with spin up. In this case, a virtual Andreev reflection will occur if $\theta_{FN}>\sin^{-1}(k_F^{\downarrow}/k_F^{\uparrow})$, where the x-component of the wave vector in the AR process becomes purely imaginary and so the AR quasiparticle can not propagate. [13,14] Further, as $\theta_{FN}>\sin^{-1}(k_F/k_F^{\uparrow})$, the x-component of the wave vector in either ELQ or HLQ transmission also becomes purely imaginary, so that a total reflection occurs and the net current from NM to SC vanishes. There is an opposite result, $\theta_{FN}>\theta_S>\theta_{FA}$, for the incident electrons with spin down. In this case, neither virtual AR nor total reflection can take place.

Figure 1b shows four types of quasiparticle injection processes in the NM/FM/SC tunnel junction: electron (I) and hole (II) incident on the NM/FM interface from NM, and ELQ (III) and HLQ (IV) incident on the FM/SC interface from SC. In the middle FM film between two δ potential barrier, the AR at the FM/SC interface and the NR in the two interfaces give rise to mutil-reflected processes of electrons with spin-σ and holes with spin-$\overline{\sigma}$. At the same time, they can transmit into NM or SC, as shown in Figure 1b. With general solutions of BdG equations (1, 2), the wave functions in NM, FM and SC regions can be obtained. Owing to translational invariance in the directions parallel to the interface, the wave function can be written as $\phi(x)\exp(\mathrm{i}\mathbf{k}_{\parallel}\cdot\mathbf{r}_{\parallel})$ where $\mathbf{k}_{\parallel}$ and $\mathbf{r}_{\parallel}$ are the wave vector and coordinate vector parallel to the interface, respectively, $|\mathbf{k}_{\parallel}|=k\sin\theta_i$ with $i=N,FN,FA,S$. As an example, for process I the wave functions in different regions are given by

$$\phi_{I\sigma}^{NM}(x)=\begin{pmatrix}1\\0\end{pmatrix}\mathrm{e}^{\mathrm{i}k_{Fx}x}+b_1^{\sigma}\begin{pmatrix}1\\0\end{pmatrix}\mathrm{e}^{-\mathrm{i}k_{Fx}x}+a_1^{\overline{\sigma}}\begin{pmatrix}0\\1\end{pmatrix}\mathrm{e}^{\mathrm{i}k_{Fx}x} \quad (3)$$

for $x\le -L/2$,

$$\phi_{I\sigma}^{FM}(x)=c_1^{\sigma}\begin{pmatrix}1\\0\end{pmatrix}\mathrm{e}^{\mathrm{i}k_{ex}^{\sigma}x}+d_1^{\overline{\sigma}}\begin{pmatrix}0\\1\end{pmatrix}\mathrm{e}^{-\mathrm{i}k_{hx}^{\overline{\sigma}}x}+e_1^{\sigma}\begin{pmatrix}1\\0\end{pmatrix}\mathrm{e}^{-\mathrm{i}k_{ex}^{\sigma}x}+f_1^{\overline{\sigma}}\begin{pmatrix}0\\1\end{pmatrix}\mathrm{e}^{\mathrm{i}k_{hx}^{\overline{\sigma}}x} \quad (4)$$

for $-L/2\le x\le L/2$, and

$$\phi_{I\sigma}^{SC}(x)=g_1^{\sigma}\begin{pmatrix}u\\v\end{pmatrix}\mathrm{e}^{\mathrm{i}q_{ex}x}+h_1^{\overline{\sigma}}\begin{pmatrix}v\\u\end{pmatrix}\mathrm{e}^{-\mathrm{i}q_{hx}x}. \quad (5)$$

for $x\ge L/2$. Here $q_{e(h)x}=k_{Fx}+(-)m\Omega/\hbar^2 k_{Fx}$, $k_{ex}^{\sigma}=k_{Fx}^{\sigma}+mE/\hbar^2 k_{Fx}^{\sigma}$, $k_{hx}^{\overline{\sigma}}=k_{Fx}^{\overline{\sigma}}-mE/\hbar^2 k_{Fx}^{\overline{\sigma}}$, with $k_{Fx}=k_F\cos\theta_i$, and $k_{Fx}^{\sigma}=k_F^{\sigma}\cos\theta_i$. $u=\sqrt{(1+\Omega/E)/2}$, and $v=\sqrt{(1-\Omega/E)/2}$ with $\Omega=\sqrt{E^2-\Delta_0^2}$. All the coefficients $a_1^{\overline{\sigma}}$, b_1^{σ}, c_1^{σ}, $d_1^{\overline{\sigma}}$, e_1^{σ}, $f_1^{\overline{\sigma}}$, g_1^{σ}, and $h_1^{\overline{\sigma}}$ can be determined by matching the boundary conditions at $x=-L/2$: $\psi_{I\sigma}^{NM}(-L/2)=\psi_{I\sigma}^{FM}(-L/2)$, $[\partial\psi_{I\sigma}^{NM}(x)/\partial x]_{x=-L/2}=[\partial\psi_{I\sigma}^{FM}(x)/\partial x]_{x=-L/2}+2k_{Fx}Z_1\psi_{I\sigma}^{NM}(-L/2)$, and at $x=L/2$: $\psi_{I\sigma}^{FM}(L/2)=\psi_{I\sigma}^{SC}(L/2)$, $[\partial\psi_{I\sigma}^{FM}(x)/\partial x]_{x=L/2}=[\partial\psi_{I\sigma}^{SC}(x)/\partial x]_{x=L/2}+2k_{Fx}Z_2\psi_{I\sigma}^{FM}(L/2)$, where $Z_1=Z_{01}/\cos\theta_N$ and $Z_2=Z_{02}/\cos\theta_N$ with $Z_{01}=mU_1/(\hbar^2 k_F)$ and $Z_{02}=mU_2/(\hbar^2 k_F)$ as the dimensionless barrier strength at the left and right interfaces. The wave functions for the other three types of quasiparticle injection processes can be obtained in a similar way.

The next step is to construct the Nambu spinor Green's functions [18] in the NM/FM/SC structure. With the wave functions $\phi_{i\sigma}(x)$ (i =I, II, III, IV, and $\sigma=\uparrow,\downarrow$) and carrying out a little tedious calculation [19], we get diagonal and off-diagonal components of the 2×2 retarded Green's functions as

$$G_r^{\sigma+}(x,x,k_{\parallel},E)_{11}=\frac{-\mathrm{i}mE}{2\hbar^2 k_{ex}^{\sigma}q_{ex}q_{hx}\Omega}[(t_1c_4^{\sigma}+t_2c_3^{\sigma})+(t_1e_4^{\sigma}+t_2e_3^{\sigma})\mathrm{e}^{\mathrm{i}2k_{ex}^{\sigma}x}+(t_3e_4^{\sigma}+t_4e_3^{\sigma})+(t_3c_4^{\sigma}+t_4c_3^{\sigma})\mathrm{e}^{-\mathrm{i}2k_{ex}^{\sigma}x}], \quad (6)$$

$$G_r^{\sigma+}(x,x,k_{\parallel},E)_{12}=\frac{-\mathrm{i}mE}{2\hbar^2 k_{ex}^{\sigma}q_{ex}q_{hx}\Omega}\Big[(t_1f_4^{\overline{\sigma}}+t_2f_3^{\overline{\sigma}})\mathrm{e}^{\mathrm{i}(k_{ex}^{\sigma}-k_{hx}^{\overline{\sigma}})x}+(t_1d_4^{\overline{\sigma}}+t_2d_3^{\overline{\sigma}})\mathrm{e}^{\mathrm{i}(k_{ex}^{\sigma}+k_{hx}^{\overline{\sigma}})x}+(t_3d_4^{\overline{\sigma}}+t_4d_3^{\overline{\sigma}})\mathrm{e}^{-\mathrm{i}(k_{ex}^{\sigma}-k_{hx}^{\overline{\sigma}})x}+(t_3f_4^{\overline{\sigma}}+t_4f_3^{\overline{\sigma}})\mathrm{e}^{-\mathrm{i}(k_{ex}^{\sigma}+k_{hx}^{\overline{\sigma}})x}\Big], \quad (7)$$

in the FM, and

$$G_r^{\sigma+}(x,x,k_\parallel,E)_{11} = -\frac{\mathrm{i}mE}{\hbar^2 q_{ex} q_{hx} \Omega} \times \Big[q_{hx}(1+b_3^\sigma \mathrm{e}^{2\mathrm{i}q_{ex}x})u^2 + q_{ex}a_4^\sigma \mathrm{e}^{\mathrm{i}(q_{ex}-q_{hx})x}uv + q_{ex}(1+b_4^{\overline{\sigma}}\mathrm{e}^{-2\mathrm{i}q_{hx}x})v^2 + q_{hx}a_3^{\overline{\sigma}}\mathrm{e}^{\mathrm{i}(q_{ex}-q_{hx})x}uv \Big], \quad (8)$$

$$G_r^{\sigma+}(x,x,k_\parallel,E)_{12} = -\frac{\mathrm{i}mE}{\hbar^2 q_{ex} q_{hx} \Omega} \times \Big[q_{hx}(1+b_3^\sigma \mathrm{e}^{2\mathrm{i}q_{ex}x})uv + q_{ex}a_4^\sigma \mathrm{e}^{\mathrm{i}(q_{ex}-q_{hx})x}v^2 + q_{ex}(1+b_4^{\overline{\sigma}}\mathrm{e}^{-2\mathrm{i}q_{hx}x})vu + q_{hx}a_3^{\overline{\sigma}}\mathrm{e}^{\mathrm{i}(q_{ex}-q_{hx})x}u^2 \Big], \quad (9)$$

in the SC. Here $t_1 = q_{ex}x_4 v\mathrm{e}^{-\mathrm{i}(k_{ex}^\sigma+q_{hx})L/2}$, $t_2 = q_{hx}x_5 u\mathrm{e}^{-\mathrm{i}(k_{ex}^\sigma-q_{ex})L/2}$, $t_3 = q_{ex}x_1 v\mathrm{e}^{\mathrm{i}(k_{ex}^\sigma-q_{hx})L/2}$, $t_4 = q_{hx}x_2 u\mathrm{e}^{\mathrm{i}(k_{ex}^\sigma+q_{ex})L/2}$, with $x_1 = k_{ex}^\sigma + q_{hx} - \mathrm{i}2k_{Fx}Z_2$, $x_2 = k_{ex}^\sigma - q_{ex} - \mathrm{i}2k_{Fx}Z_2$, $x_4 = k_{ex}^\sigma - q_{hx} + \mathrm{i}2k_{Fx}Z_2$, $x_5 = k_{ex}^\sigma + q_{ex} + \mathrm{i}2k_{Fx}Z_2$.

From the Green's function obtained above, the pair potential can be recalculated, yielding

$$\Delta(x) = \lambda^*(x)F(x). \quad (10)$$

Here $\lambda^*(x) = (\lambda - \mu^*)/(1+\lambda)$ with λ the dimensionless electron-phonon coupling constant and μ^* the Coulomb pseudopotential [11]. λ and μ^* are taken equal to the bulk value in SC and zero in FM. $F(x)$ is the superconducting order parameter, which is determined by the off-diagonal component of the Green's function ($x = x'$),

$$F(x) = (1/\pi)\sum_{k_\parallel,\sigma}\int_0^\infty \mathrm{d}E \mathrm{Im}\left[G_r^\sigma(x,x,k_\parallel,E)\right]_{12}. \quad (11)$$

The calculated result for spatial dependence of $F(x)$ in the NM/I/FM/SC structure is plotted in Figure 2. On the SC side, due to the pair-breaking effect of spin-polarized electron incident from FM, the superconducting order parameter is reduced near the FM/SC interface and recovers its bulk value with the distance from the interface increased beyond the coherent length ξ_S in SC. The recalculated pair potential $\Delta(x)$ in SC is equal to the bulk λ^* times $F(x \geq L/2)$ given in Figure 2, and that in FM is zero because $\lambda^* = 0$ there. This potential is not very different from the assumed one, $\Delta(x) = \Delta_0\Theta(x)$, indicating that the potential is now nearly self-consistent. On the FM side, there appears an oscillating superconducting order parameter from positive ("0" state) to negative ("π" state), its amplitude being gradually decreased with leaving away from the FM/SC interface. The oscillation period is of the same order of magnitude as the coherence length $\xi_F = \hbar v_F/2h_0$ in FM. It is much shorter than the coherence length $\xi_S = \hbar v_F/2\Delta_0$ in SC. This is the reason that there exists a change of $F(x)$ from positive to negative in the FM/SC proximity structure, as shown in Figure 2;

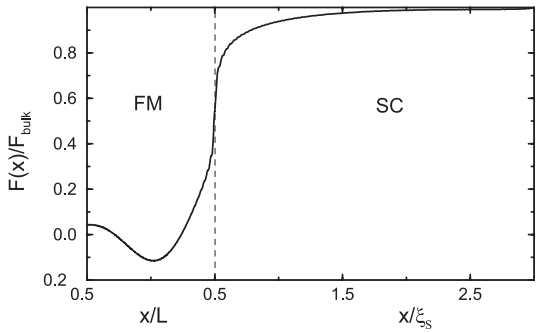

Fig. 2. Spatial variation of superconducting order parameter $F(x)$ in FM and SC. Here $L = 2.0\xi_F$, $\xi_F = \hbar v_F/2h_0$ and $\xi_S = \hbar v_F/2\Delta_0$ with $Z_{01} = 3$, $Z_{02} = 0.22$, $h_0 = 15\Delta_0$ and $E_F = 1000\Delta_0$ taken.

while such a change can not seen in an NM/SC structure due to too long oscillation period compared with the damping length there. The superconducting order parameter describes the number of Cooper pairs in the condensate. The existence of superconducting order parameter in FM indicates that there are finite population of Cooper pairs near the FM/SC interface. As the Cooper pairs are injected from SC to FM *via* the interface, they are not instantaneously broken and can survive for a traveled length on the order of several ξ_F. Such spatially modulated superconductivity in FM is indicative of coexistence of superconductivity and ferromagnetism within the FM film. However, this coexistence induced by the proximity effect is quite different from that in a bulk FM.

The local DOS of the quasiparticles is proportional to the imaginary part of the 11 component of the 2×2 retarded Green function ($x = x'$),

$$N(x,E) = (-1/\pi)\sum_{k_\parallel,\sigma}\mathrm{Im}\left[G_r^\sigma(x,x,k_\parallel,E)\right]_{11}. \quad (12)$$

Figure 3 shows the calculated results of energy dependence of the induced superconducting DOS in FM at the I/FM interface ($x = -L/2$), in which the DOS has been normalized by that when the SC is at its normal state ($\Delta_0 = 0$). We see that for the thickness of the FM film equal to $0.6\xi_F$ and $1.2\xi_F$, the DOS has a minimum at the Fermi level ($E = 0$) and a maximum (peak) at the energy gap edge ($E = \Delta_0$). The shape of the DOS is somewhat like that in SC, corresponding to the "0" state, even though the present DOS fluctuates within a very narrow range. As the thickness of the FM film is increased to be $2.0\xi_F$ and $2.3\xi_F$, the DOS is reversed, exhibiting a maximum at $E = 0$ and a minimum (dip) at $E = \Delta_0$, which is a feature of "π"-state superconductivity. This reversion of DOS arises from spatial dependence of macroscopic phase for the Cooper pairs in FM, it corresponds just to the change of the induced superconducting order parameter $F(x)$ from positive to negative in Figure 2. It is interesting to see that for $L = 1.8\xi_F$, the peaks at $\mid E \mid = \Delta_0$ become very small, while a small peak appears at the center of the concave-down curve within the energy gap. This behavior indicates a typical crossover from the "0" state to the "π"

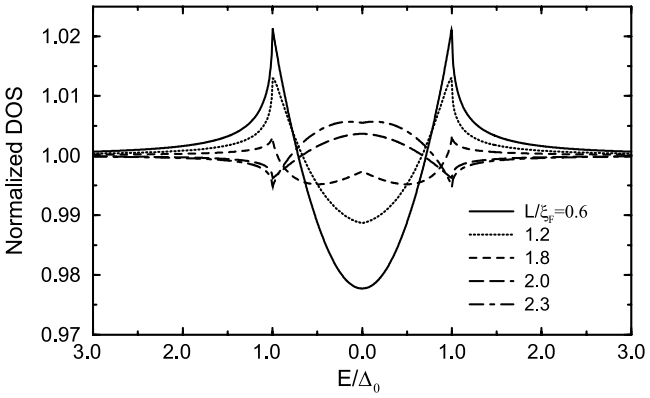

Fig. 3. Energy dependence of DOS in FM at $x = -L/2$ for different L. It is gradually reversed from "0 state" to "π state" with increasing the thickness of the FM film. The parameters used are the same as in Figure 2.

one. In the present calculation the parameters are taken to be bulk values of Nb and PdNi: $E_F = 1000\Delta_0 = 1.4$ eV, $h_0 = 15$ meV, and $\xi_F = 40$ Å. The other parameters are $Z_{01} = 3$ and $Z_{02} = 0.22$. The large value for Z_{10} simulates the insulating Al_2O_3 layers at the Al/PdNi interface and the small value for Z_{20} is well consistent with a very low PdNi/Nb interface resistance. With these reasonable parameters the calculated results for $L/\xi_F = 1.2$ and 2.0 can be well consistent with differential conductance *vs.* bias for two $Al/Al_2O_3/PdNi/Nb$ tunnel junction corresponding to $L = 50$ and $75\mathring{A}$ of PdNi, respectively (see Fig. 2a of Ref. [6]). In particular, the peak and dip behavior of the induced superconducting DOS at $\mid E \mid = \Delta_0$ is reproduced.

The agreement between the obtained result and the experimental data [6] is reasonable, because the model system used here has the same structure as in the experiment. However, a simplified model system with the finite FM film replaced by a semifinite FM [10] was also able to reproduce the experimental data by adjusting the barrier parameter of the FM/SC interface, indicating that the simplified model had captured the essential physics of such a proximity structure. The superconducting order parameter and the DOS with superconducting feature originate from the injection of the Cooper pairs from SC to FM, and their damped oscillatory behavior arises from the quantum interference between electrons (holes) and the Andreev reflected holes (electrons). As a result, the proximity effect does not depend on whether the FM is semi-infinite or finite.

On the SC side, it is found that there is finite DOS for $\mid E \mid < \Delta_0$ near the FM/SC interface, such as at $x/\xi_S = 0.1$ and 1.0 with $\xi_S = \hbar v_F/2\Delta_0$ the coherent length of the SC, as shown in Figures 4a and b. The nonvanishing DOS within the energy gap indicates gapless superconductivity induced by the proximity effect. More importantly, the DOS is spin dependent, as shown by dashed and dotted lines in Figure 4. From the different DOS for spin-up and spin-down electrons, it follows that the induced ferromagnetism appears in SC near the interface,

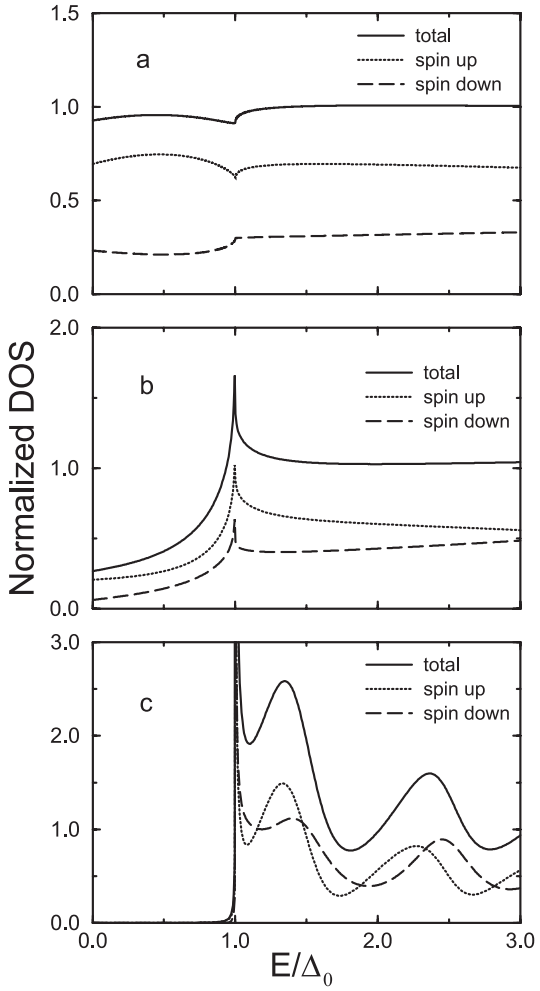

Fig. 4. Superconducting DOS in SC at $x/\xi_S = 0.1$ (a), 1.0 (b), and 2.5 (c). Solid, dotted, and dashed line lines correspond to the total DOS, spin-up and spin-down DOS, respectively. Here $L/\xi_F = 1.2$ and the other parameters are the same as in Figure 2.

which is attributed to the injection of spin-polarized electron from FM. This injection gives rise to the pair-broken effect in SC, resulting in the reduction of the superconducting order parameter and gapless superconductivity near the FM/SC interface. With increasing distance away from the interface ($x = 2.5\xi_S$ in Fig. 4c), the DOS recovers vanishing within the energy gap, as in the bulk SC, although there exist some oscillating behavior in the spin-up and down DOS for $\mid E \mid > \Delta_0$.

In summary, we have applied the Nambu spinor Green's function approach and BTK theory to study the proximity effect in NM/I/FM/SC junctions, in particular the coexistence of ferromagnetism and superconductivity in the regime near the FM/SC interface. On the SC side, the injection of spin-polarized electrons from FM results in not only novel gapless superconductivity, but also spin-dependent DOS. On the FM side, the injection of the Cooper pairs from SC, together with the exchange field of the FM, leads to a damped oscillation of the

superconducting order parameter and the DOS with superconducting feature. This DOS exhibits peak at the energy gap edge for the "0 state" and dip at the same energy for the "π state". The calculated results are quantitatively consistent with the tunneling conductance spectra in $Al/Al_2O_3/PdNi/Nb$ tunnel junctions.

This work is supported by the National Natural Science Foundation of China under Grant No. 10174011. Part of this work was done during D.Y. Xing's visit to the Department of Physics at the Chinese University of Hong Kong through the "C.N. Yang Visiting Professor Program", and he wish to thank the Physics Department for its hospitality and support.

References

1. M.A. Clogston, Phys. Rev. Lett. **9**, 266 (1962)
2. B.S. Chandrasekhar, Appl. Phys. Lett. **1**, 7 (1962)
3. A.A. Abrikosov, L.P. Gorkov, Zh. Eksp. Theo. Fiz. **39**, 1781 (1960) [Sov. Phys. JETP **12**, 1243 (1961)]
4. P. Fulde, A. Ferrel, Phys. Rev. **135**, A550 (1964)
5. A. Larkin, Y. Ovchinnikov, Sov. Phys. JETP **20**, 762 (1965)
6. T. Kontos, M. Aprili, J. Lesueur, X. Grison, Phys. Rev. Lett. **86**, 304 (2001)
7. V.V. Ryazanov *et al.*, Phys. Rev. Lett. **86**, 2427 (2001)
8. A. Buzdin, Phys. Rev. B **62**, 11377 (2000)
9. M. Zareyan, W. Belzig, Yu. V. Nazarov, Phys. Rev. Lett. **86**, 308 (2001)
10. G.Y. Sun, D.Y. Xing, J.M. Dong, M. Liu, Phys. Rev. B **65**, 174508 (2002)
11. W.L. McMillan, Phys. Rev. **175**, 559 (1968)
12. G.E. Blonder, M. Tinkham, T.M. Klapwijk, Phys. Rev. B **25**, 4515 (1982)
13. I. Zutic, O.T. Valls, Phys. Rev. B **60**, 6230 (1999)
14. S. Kashiwaya, Y. Tanaka, N. Yoshida, M. Beasley, Phys. Rev. B **60**, 3572 (1999)
15. A.A. Golubov, M.Yu. Kupriyanov, J. Low Temp. Phys. **70**, 83 (1988); Sov. Phys. JETP **69**, 805 (1989)
16. W. Belzig, C. Bruder, G. Schon, Phys. Rev. B **54**, 9443 (1996)
17. A.V. Andreev, A. Buzdin, R.M. Osgood III, Phys. Rev. B **43**, 10124 (1991)
18. Y. Nambu, Phys. Rev. **117**, 648 (1960)
19. S. Kashiwaya, Y. Tanaka, Rep. Prog. Phys. **63**, 1641 (2000)